Mon. Not. R. Astron. Soc. **000**, 000–000 (0000) Printed 21 November 2001 (MN LATEX style file v1.4)

An electrically powered binary star?

Kinwah Wu[1,2], Mark Cropper[2], Gavin Ramsay[2] and Kazuhiro Sekiguchi[3]
[1] *Research Centre for Theoretical Astrophysics, School of Physics A28, University of Sydney, NSW 2006, Australia*
[2] *Mullard Space Science Laboratory, University College London, Holmbury St. Mary, Dorking, Surrey, RH5 6NT*
[3] *Subaru Telescope, National Astronomical Observatory of Japan, 650 North A'ohoku Place, Hilo, HI 96720, USA*

Received:

ABSTRACT

We propose a model for stellar binary systems consisting of a magnetic and a non-magnetic white-dwarf pair which is powered principally by electrical energy. In our model the luminosity is caused by resistive heating of the stellar atmospheres due to induced currents driven within the binary. This process is reminiscent of the Jupiter-Io system, but greatly increased in power because of the larger companion and stronger magnetic field of the primary. Electrical power is an alternative stellar luminosity source, following on from nuclear fusion and accretion. We find that this source of heating is sufficient to account for the observed X-ray luminosity of the 9.5-min binary RX J1914+24, and provides an explanation for its puzzling characteristics.

Key words: stars: binaries: close — stars: magnetic field — stars: individual: RX J1914+24 — X-rays: stars

1 INTRODUCTION

It has been observed directly by the *Hubble Space Telescope* that the movement of Io through Jupiter's magnetic field causes heating in the Jovian atmosphere (Clarke et al. 1996). This is because a conducting body transversing a magnetic field produces an induced electric field. When the circuit is closed, a current will be set up, resulting in resistive dissipation. The Jupiter-Io system therefore operates as a unipolar inductor (Paddington & Drake 1968; Goldreich & Lynden-Bell 1969). Another potential cosmic unipolar inductor could be a planet orbiting around a magnetic white dwarf (Li, Ferrario & Wickramasinghe 1998). These systems have a similar configuration, with the differences being their orbital period and separation, the masses and radii of the two components, and the magnetic moment of the magnetic object.

We propose that binary stars consisting of a magnetic and a non-magnetic white dwarf can also be cosmic unipolar inductors (Fig. 1). Close binaries of this type can have short periods and secondaries larger than planet-sized bodies. Provided that the spin of the magnetic white dwarf and the orbital rotation are not synchronised (so that the secondary is in motion relative to the magnetic field) and that the density of the plasma between the white dwarfs is high enough, unipolar induction will operate efficiently.

Gravitational waves carry away the orbital angular momentum efficiently from a short-period (<2 hr) binary system but not the stellar spin momenta directly. In a magnetic and non-magnetic white-dwarf pair with only the non-magnetic star tidally locked, the magnetic star will be spun up retrogradely in the orbital rest frame as the binary orbit shrinks. Alternatively, the magnetic white dwarf could be spun up by accretion in a previous epoch in which mass transfer occurred, so that it has a spin faster than the orbital rotation. Asynchronous rotation can therefore occur as long as a stellar component is not tidally or otherwise locked.

The dissipative power of a white dwarf–planet pair with an orbital period $P = 10$ hr is estimated to be $\sim 10^{29}$erg s^{-1} (Li, Ferrario & Wickramasinghe 1998). The output of a binary white-dwarf pair with a period of tens of minutes will be significantly higher and should have detectable observational consequences.

In this paper, a simple model for a unipolar inductor consisting of a magnetic and a non-magnetic white-dwarf pair in a close orbit is presented. The basic features of these binaries and their observational properties are discussed. We propose that the short-period soft X-ray source RX J1914+24 (Cropper et al. 1998; Ramsay et al. 2000a) is a candidate unipolar inductor consisting of a magnetic and non-magnetic white-dwarf pair.

2 WHITE-DWARF PAIRS AS COSMIC UNIPOLAR INDUCTORS

When a non-magnetic conductor of linear size R transversing a magnetic field $\vec{B}$ with a velocity $\vec{v}$, the induced e.m.f. across the conductor is $\Phi \sim R|\vec{E}|$, where $\vec{E} = (\vec{v} \times \vec{B})/c$ (c is the speed of light). Thus, the corresponding e.m.f. across a non-magnetic white dwarf in orbit with a magnetic white

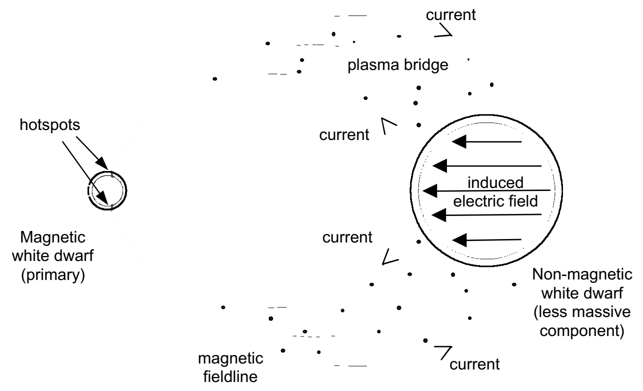

Figure 1. A schematic illustration of a unipolar inductor consisting of a magnetic and non-magnetic white-dwarf pair in a close binary orbit.

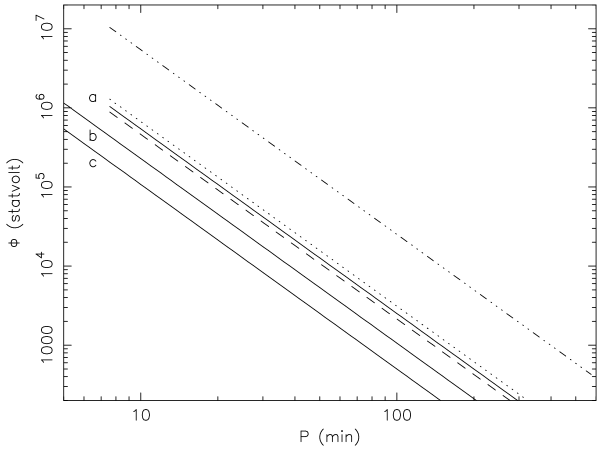

Figure 2. The induced e.m.f. across the non-magnetic secondary white dwarf as a function of orbital period for binaries with various parameters. Solid lines a, b and c correspond to systems with a primary magnetic white dwarf of 1.0 $M_\odot$ with a spin 1 part of 1000 deviated from synchronous rotation with the orbit. The masses of the secondaries in these systems are 0.1, 0,5 and 1.0 $M_\odot$ respectively. The dotted line corresponds to systems consisting of a 0.1-$M_\odot$ non-magnetic white dwarf, and a 0.7-$M_\odot$ magnetic white dwarf with 1 part of 1000 off spin-orbit synchronism; and the dashed line corresponds to similar systems but with a 1.3-$M_\odot$ primary magnetic white dwarf. Systems with magnetic and non-magnetic white-dwarf pairs of mass 1.0 and 0.5 $M_\odot$ and spin-orbital asynchronism of 1 part in 100 for the magnetic white dwarf is represented by the dot-dashed line. The magnetic moments of the systems are fixed to be 10^{32} G cm^3.

dwarf is

$$\begin{aligned}\Phi &\approx \frac{2\pi}{c}\left(\frac{\mu_1 R_2}{a^2 P}\right)(1-\alpha) \\ &= \left(\frac{\mu_1 R_2}{c}\right)\left(\frac{2\pi}{P}\right)^{7/3}(1-\alpha)\big[GM_1(1+q)\big]^{-2/3}, \quad (1)\end{aligned}$$

where G is the gravitational constant, q ($\equiv M_2/M_1$) is the ratio of the non-magnetic to the magnetic white dwarf mass, R_2 and R_1 are the radii of the non-magnetic and the magnetic white dwarf respectively, μ_1 is the magnetic moment of the magnetic white dwarf. The degree of asynchronism α is defined as the ratio of the spin angular speed of the magnetic white dwarf ω_1 to the orbital angular speed ω_o $(= 2\pi/P)$. (Here and elsewhere, we consider that the anti-clockwise direction is positive.) We show in Figure 2 the induced e.m.f. for different system parameters. The induced e.m.f. depends strongly on the orbital period, the degree of spin-orbit synchronism, and the mass (radius) of the non-magnetic white dwarf. The dependence of the mass of the magnetic white dwarf is weaker.

If the space between the white dwarfs is filled with plasma, the induced e.m.f. will drive currents along the magnetic field lines connecting the two white dwarfs. Because there is substantial resistance in the white-dwarf atmosphere, the white dwarfs act as the dissipative components in this electrical circuit. The total electrical power dissipation in the two white dwarfs is

$$\begin{aligned}W &= I^2(\mathcal{R}_1+\mathcal{R}_2) \\ &= \Phi^2/(\mathcal{R}_1+\mathcal{R}_1)\ , \quad (2)\end{aligned}$$

where I is the total current, and $\mathcal{R}_1$ and $\mathcal{R}_2$ are the effective resistance of the magnetic and the non-magnetic white dwarfs respectively. An object with a length L and an area A has a resistance $\mathcal{R} = L/A\sigma$ (where σ is conductivity). Therefore, the ratio of the effective resistances of the white dwarfs is

$$\frac{\mathcal{R}_1}{\mathcal{R}_2} \sim \left(\frac{\sigma_2}{\sigma_1}\right)\left(\frac{R_2^2}{fR_1^2}\right)\left(\frac{\Delta h_1}{\Delta h_2}\right)\ , \quad (3)$$

where σ_1 and σ_2 are the conductivity of the magnetic and the non-magnetic white dwarf respectively, Δh_1 and Δh_2 are the thickness of the dissipative surface layers of the white dwarfs, and f is the fractional effective area of the magnetic poles (hot spots) on the surface of the magnetic white dwarf. As $f \ll 1$ (see Appendix A), the effective resistance of the magnetic white dwarf is significantly larger than the non-magnetic white dwarf.

As the currents pass through both white dwarfs, the ratio of the power dissipation in the magnetic primary to that of the non-magnetic secondary is $W_1/W_2 = \mathcal{R}_1/\mathcal{R}_2$. Taking account of the geometry of the current loops, we obtain

$$\frac{W_1}{W_2} \approx \beta\left(\frac{\sigma_2}{\sigma_1}\right)\left(\frac{R_2}{\Delta R_2}\right)\left[\frac{G(M_1+M_2)}{R_1^3}\left(\frac{P}{2\pi}\right)^2\right]^{1/2} ; \quad (4)$$

$$\mathcal{R}_1 \approx \frac{1}{2\sigma_1}\left(\frac{H}{\Delta d}\right)\left(\frac{a}{R_1}\right)^{3/2}\frac{\mathcal{J}(e)}{R_2}\ ; \quad (5)$$

$$\mathcal{R}_2 \approx \frac{4}{\pi\sigma_2}\left(\frac{\Delta R_2}{R_2^2}\right) \quad (6)$$

(see Appendices A and B for details), where ΔR_2 is the thickness of the secondary's atmosphere and β is a structure factor of the order of unity. The factor $\mathcal{J}(e)$ depends of the radii of the white dwarfs relative to the orbital separation. Its value is of the order of unity for white-dwarf pairs with orbital periods less than an hour.

The conductivity of plasma of an electron temperature

T_e is given by

$$\sigma = \gamma\left(\frac{2^{5/2}}{\pi^{3/2}}\right)\frac{(kT_e)^{3/2}}{m_e^{1/2}Ze^2\ln\Lambda}\ , \tag{7}$$

(Spitzer & Härm 1953) where k is the Boltzmann constant, T_e is the electron temperature, m_e is the electron mass, e is the electron charge, Z is the ion charge number, and $\ln\Lambda$ is the Coulomb logarithm. The factor γ depends on the ion charge number Z, which has values between 0.6 ($Z = 1$) and 1 ($Z \to \infty$) (see Alfvén & Fälthammar 1963). For a white-dwarf atmosphere with $T_e \sim 10^5$ K, the conductivity $\sigma \sim 10^{13} - 10^{14}$ esu. Since the conductivities of the atmospheres of white dwarfs are similar to each other, the majority of the electrical power will be dissipated in small regions at the footpoints of the current-carrying field lines on the surface of the magnetic white dwarf.

3 ENERGY AND ANGULAR-MOMENTUM CONSERVATION

3.1 Power dissipation

If the degree of spin-orbit asynchronism $(1-\alpha)$ is specified, the total power dissipation of the binary can be calculated directly using equations (1), (2), (4) and (5). We show in Figure 3 the total power dissipation W as a function of the orbital period P, for systems with different primary and secondary white-dwarf masses M_1 and M_2. The general trend of the dependence of W on the system parameters is as follows: (i) the power dissipation W is larger for larger degree of spin-orbit asynchronism; (ii) W increases when P decreases; (iii) the larger is the radius of the non-magnetic white dwarf R_2, the larger W will be; and (iv) W decreases slightly when M_1 increases. Moreover, provided that there is a slight spin-orbit asynchronism (1 part in 1000 is sufficient) and that the asynchronously rotating white dwarf has a moderate magnetic moment ($\sim 10^{32}$ G cm^3), the electrical power dissipation of the systems can reach the solar luminosity $L_\odot$ (3.9×10^{33} erg s^{-1}), when the orbital period is short enough ($\lesssim$10 min). Clearly, the electrical power generated by these close binaries is substantially larger than the expected intrinsic luminosities of the white-dwarf components, which is $\ll L_\odot$.

It is worth noting that most of the luminosity originates from the two hot spots near the magnetic poles at the surface of the magnetic white-dwarf. If the footpoints of the current-carrying fieldlines remain fixed with respect to the secondary, as in the Jupiter-Io system (Clarke et al. 1996), asynchronous rotation will not manifest itself in orbital-period changes, but will possibly be visible through changes in the spot latitudes if the dipole is not aligned with the spin axis.

3.2 Spin-orbit coupling

The consequence of the energy dissipation is the creation of a Lorentz torque, which tends to synchronise the spin of the magnetic white dwarf with the spin of the non-magnetic white dwarf, and hence with the orbital rotation. Thus, through spin-orbit coupling, energy and angular momentum can also be exchanged between orbit and the white dwarfs.

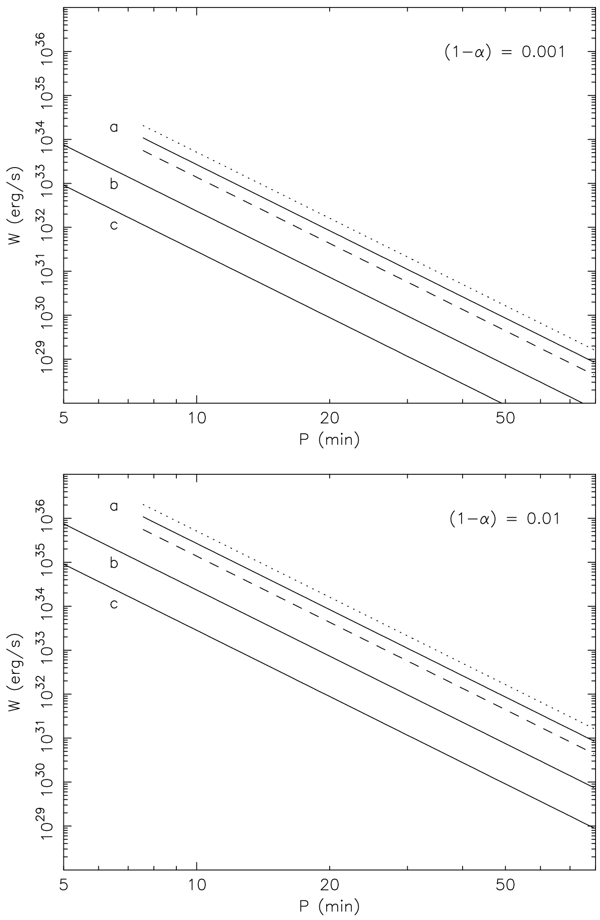

Figure 3. The total electrical power dissipation as a function of orbital period. The degree of deviation from spin-orbit asynchronism $(1-\alpha)$ is 1 part in 1000 in the top panel and 1 part in 100 in the bottom panel. As in Fig. 2 the solid lines a, b and c correspond to systems with a non-magnetic white-dwarf secondary of 0.1, 0.5 and 1.0 M$_\odot$. The mass of the magnetic primary is 1.0 M$_\odot$. The dotted line corresponds to systems consisting of a 0.7-M$_\odot$ magnetic white dwarf and a 0.1-M$_\odot$ non-magnetic white dwarf, and the dashed line corresponds to systems consisting of a 1.3-M$_\odot$ magnetic white dwarf and a 0.1-M$_\odot$ non-magnetic white dwarf. The magnetic moment of the primary is fixed to be 10^{32} G cm^3.

If the secondary white dwarf is tidally locked to the orbit, as assumed in our model, the evolution of the spin of the magnetic primary white dwarf ω_1, the orbital rotation ω_o, and the degree of synchronisation is governed by the equations:

$$\frac{\dot\omega_1}{\omega_1} = \frac{W}{\alpha(1-\alpha)I_1\omega_o^2}\ ; \tag{8}$$

$$\frac{\dot\omega_o}{\omega_o} = \frac{1}{g(\omega_o)}\left[\dot E_{\rm ex} - \frac{W}{(1-\alpha)}\right]\ ; \tag{9}$$

$$\frac{\dot\alpha}{\alpha} = -\frac{1}{g(\omega_o)}\left[\dot E_{\rm ex} - \frac{W}{(1-\alpha)}\left(1+\frac{g(\omega_o)}{\alpha I_1\omega_o^2}\right)\right] \tag{10}$$

(see Appendices C, D and E), where

$$g(\omega_o) = -\frac{1}{3}\left[\frac{q^3}{(1+q)}G^2M_1^5\omega_o^2\right]^{1/3}$$

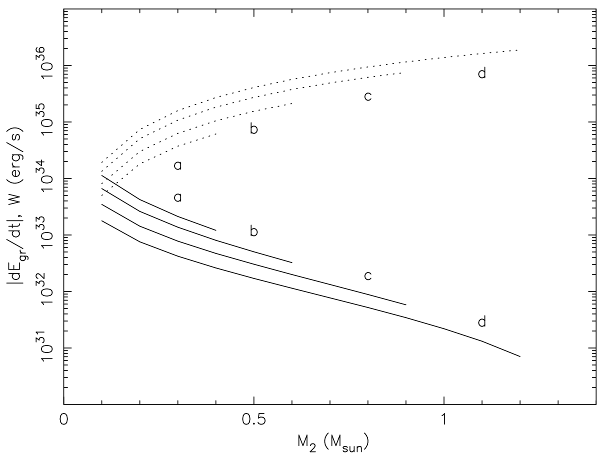

Figure 4. The total electrical power dissipation (solid lines) and the power of gravitation radiation emitted from the binary (dotted lines) as a function of mass of the non-magnetic white dwarf. The orbital period is fixed to be 9.5 min. Curves a, b, c and d correspond to systems with a 0.5, 0.7, 1.0, and 1.3-$M_\odot$ magnetic white dwarf. The magnetic moments of the white dwarfs are 10^{32} G cm^3. The spin of the magnetic white dwarf is 1 part in 1000 deviated from synchronous rotation with the orbit, i.e. $(1-\alpha) = 0.001$.

$$\times \left[1 - \frac{6}{5}(1+q)f(\omega_o)\right] . \qquad (11)$$

The term $\dot{E}_{\rm ex}$ is the energy loss due to external process (such as gravitational radiation). The factor $f(\omega_o)$ can be expressed in terms of orbital parameters, which is simply $(R_2/a)^2$. Clearly, the spin-orbit evolution is jointly determined by the rate of energy loss due to gravitation radiation $\dot{E}_{\rm gr}$ and the electrical power dissipation W.

For short-period binaries gravitational radiation is an efficient process to extract energy from the binary orbit (Paczńyski 1967; Faulkner 1971). As an illustration we show in Figure 4 the electric power dissipation W and the rate of energy loss from the orbit due to gravitation radiation $\dot{E}_{\rm gr}$ for binaries with an orbital period < 10 min and spin-orbital asynchronism of 1 part in 1000. The power loss due to gravitational radiation is generally larger than the electrical power dissipation, except for systems with a very low-mass non-magnetic white dwarf.

As $W \propto (1-\alpha)^2 > 0$ (from Equations 1 and 2), energy is extracted from the spin of the magnetic white dwarf, if it is a fast spinner $\alpha > 1$ (Equation 9). When $\alpha < 1$, energy is injected to spin up the magnetic white dwarf. Because both $\dot{E}_{\rm gr}$ and $g(\omega_o)$ are negative, when energy is extracted from the orbit to spin up the magnetic white dwarf, the orbit shrinks and the orbital angular speed increases. For white-dwarf pairs consisting of a 1.0-$M_\odot$ magnetic primary and a 0.1-$M_\odot$ secondary with a 10-min orbit and a spin-orbital asynchronism of 1 part in 1000, the typical evolutionary timescale for α is about 10^3 years. As the synchronisation timescale due to unipolar induction is significantly shorter than the timescale of the gravitational-radiation power loss, which is about 10^6 years for these systems, these systems are expected to be rare in comparison with 'ordinary' white-dwarf pairs.

3.3 Effects of the induced magnetic field

In the unipolar-inductor model that we consider above, the magnetic field generated by the currents between the white dwarfs has been neglected. Because of this induced magnetic field, the magnetic-field configuration is no longer dipolar as for the assumed intrinsic field of the primary white dwarf. As a result, the currents and the magnetic field lines are not aligned, and there will an additional drag to the motion of the secondary white dwarf. This plasma-inertia effect can be non-negligible.

The importance of plasma-inertia effects in the Jupiter-Io system was investigated by Drell, Foley & Ruderman (1965) in the linear approximation and by Neubauer (1980) using a more appropriate non-linear treatment. These studies showed that the non-alignment of the currents and magnetic field is associated with the Alfvén waves — called Alfvén wings — standing in the frame of Io, causing dissipation in the polar regions of Jupiter as well as in Io.

Here in this white-dwarf pair, the standing Alfvén waves are in the frame of the non-magnetic secondary white dwarf. The significance of the plasma-inertia effects can be expressed by the Alfvén Mach number

$$M_{\rm A} \ = \ \frac{\delta v}{v_{\rm A}} \ , \qquad (12)$$

where δv is velocity of secondary white dwarf related to the magnetosphere of the primary magnetic white dwarf, given by $\delta v \sim (1-\alpha)\pi a/P \approx 10^9\ (1-\alpha)$ cm s^{-1}, and $v_{\rm A}$ is the Alfvén speed:

$$v_{\rm A} \ = \ 1.5 \times 10^9 \left(\frac{B}{1\ {\rm kG}}\right) \left(\frac{n_{\rm e}}{10^{10}{\rm cm}^{-3}}\right)^{-1/2} {\rm cm\ s}^{-1} \ , \qquad (13)$$

($n_{\rm e}$ is the electron number density in the plasma). For the parameters of our interest, $M_{\rm A} \ll 1$ is generally satisfied, and the plasma-inertia effects can be considered as a perturbation. The results that we have obtained are therefore generally valid.

The large currents in the system can also cause significant distortion of the magnetic field near the primary magnetic white dwarf. The geometry of the energy-dissipation region and the electrical circuit of the system are therefore not as simple as described in our idealised model. A particular issue is whether or not steady currents can be maintained given the presence of a large $\vec{j} \times \vec{B}$ force, when the current and the magnetic field are not aligned. This could eventually lead to the breakdown of the circuit and quench the operation of the unipolar induction. Nevertheless, if the unipolar induction does operate, in spite of the non-alignment of current and field, the energy and angular-momentum budget should be similar to that of the unipolar-inductor model that we have presented above. (Detail investigation of the effects due to severe field distortion is beyond the scope of this paper, and will be left for future study.)

4 RX J1914+24: A POSSIBLE UNIPOLAR INDUCTOR?

We propose that the short-period binary system RX J1914+24 is electrically powered. This system emits soft X-rays which are modulated on a period of 9.5 min, and whose folded light curve is that expected from emission originating from one or two small spots. The optical/infra-red flux is also modulated only on the 9.5-min period but maximum light occurs ~ 0.4 orbital cycles earlier than the soft X-rays (Ramsay et al. 2000b).

It has been argued that the system is a magnetic white dwarf-white dwarf binary, which is synchronised by the strong magnetic interaction between the white dwarfs (Cropper et al. 1998). An accretion scenario has been proposed (Ramsay et al. 2000a), in which the optical flux is due to irradiation by the accreting material, and which can largely account for the observations. However, to explain the lack of optical polarisation (Ramsay et al. 2000a), the magnetic-field strength on the primary must either be too high or too low to be detected in the optical/infra-red. Also, a major concern is that the accretion model is unable to explain the observed lack of strong emission lines (Ramsay et al. 2000b) which result from heating of the accretion stream in mass-transfer systems.

If the secondary in RX J1914+24 fills its Roche lobe (Cropper et al. 1998), $M_2 \approx 0.1\mathrm{M}_\odot$. A Roche-lobe-filling star is more easily tidally locked into synchronous rotation with the orbit. In the unipolar-inductor model proposed above, the secondary is allowed to lie within its Roche lobe, and so this mass is a lower limit. The mass of the primary is, however, unconstrained. Based on *ROSAT* and *ASCA* measurements and an estimated distance of 200-500 pc, the deduced luminosity of RX J1914+24 is in the range 4×10^{33} to 1×10^{35} erg s^{-1} (Ramsay et al. 2000b). Provided that the spin-orbit asynchronism of the magnetic white dwarf is about 1 part in 1000 or larger, the resistive heating is sufficient to power these luminosities (See Figures 3 and 4). From Equation (4), the resistive dissipation power is estimated to be $\sim 10^{31} - 10^{32}$ erg s^{-1} in the secondary's atmosphere. The result is less sensitive to other system parameters such as the mass of the magnetic white dwarf. A comparison between the observed and predicted luminosities suggests that the secondary is 0.15 $\mathrm{M}_\odot$, and thus close to filling its Roche lobe and tidally locked.

The predicted area of each hotspot on the primary is $\sim 8 \times 10^{14}$ cm^2 (from Appendix A). If we use the observed luminosity of 10^{34} erg s^{-1} (assuming a distance $d = 300$ pc), we obtain a blackbody temperature of 50 eV, consistent with the measured value of 55 eV from the *ROSAT* and *ASCA* spectral fits (Ramsay et al. 2000b). This consistent area is corroborating evidence that the underlying geometry of the model is valid.

For a system with a 1.0-$\mathrm{M}_\odot$ primary, a 0.1-$\mathrm{M}_\odot$ secondary and an orbital period of 9.5 min, less than 1 percent of the X-ray flux emitted from the hotspots primary is intercepted by the secondary. In equilibrium, the intercepted flux will be reradiated, resulting in an increase in the luminosity of the irradiated hemisphere of the secondary. The additional luminosity arising from irradiation heating is estimated to be $\lesssim 10^{32}$ erg s^{-1}. Thus, the power of irradiative heating of the secondary is similar to the power of electrical heating. Given the fact that the two heating processes have similar efficiency, one would not expect a large temperature difference in the irradiated and the unirradiated hemisphere of the secondary. This is consistent with the observation that the amplitude of variation in the optical luminosity in RX J1914+24 is small (Ramsay et al. 2000a). Moreover, as the power of irradiative heating is of the same order of the energy flux from below the atmosphere due to resistive heating, the presence of moderate heat conduction is sufficient to maintain an approximate isothermal layer down to unit optical depth. Because of the absence of an temperature inversion layer, the secondary will not show emission lines in its spectrum: this is consistent with the lack of prominent emission lines in the optical spectrum (Ramsay et al. 2000b).

5 SUMMARY

We propose that short-period magnetic and non-magnetic white-dwarf pairs with short orbital periods (~ 10 min) are efficient cosmic unipolar inductors. Provided that the spin of the magnetic component and the orbit are not in perfect synchronism, a large e.m.f. can be produced across the non-magnetic white dwarf. The resistive dissipation in the white dwarfs is sufficient to power luminosities significantly above solar values; most power is dissipated at the hot spots on the surface of the magnetic white dwarfs, which are footpoints of the field lines connecting the two stars. Electrical power is therefore an alternative luminosity source, following on from nuclear fusion and accretion.

The X-ray source RX J1914+24 is a candidate unipolar inductors consisting of a magnetic and non-magnetic white-dwarf pair. The two small X-ray spots on the magnetic white dwarf predicted by the unipolar-inductor model are compatible with the X-ray light curve of RX J1914+24. The luminosity and temperature predicted by the model is also in agreement with the observed values derived from fits to the X-ray spectra. The model also explains the variation in the optical/infra-red luminosity, and the detection of only a single period. The variations in the long term X-ray intensity can be attributed to variations in the current flow. The two main inadequacies of the current accretion model (Ramsay et al. 2000a) — the lack of any polarised flux and the lack of any detectable line emission (Ramsay et al. 2000b) are naturally explained.

ACKNOWLEDGMENTS

KW acknowledges the support from the Australian Research Council through an ARC Australian Research Fellowship, and from the UK PPARC for a Visiting Fellowship Grant at MSSL, when much of this work was carried out. We thank Jan Kuijpers, Jianke Li, Qinghuan Luo and Mark Wardle for discussions and critical reading of the manuscript. We also thank Jan Kuijpers and Don Melrose for pointing to our attention of effects due to the Alfvén wings.

REFERENCES

Alfvén, H., Fälthammar, C.-G., 1963, Cosmic Electrodynamics, Oxford University Press, London

Clarke, J. T. et al., 1996, Science, 274, 404
Cropper, M., Harrop-Allin, M. K., Mason, K. O., Mittaz, J. P., Potter, S. B., Ramsay, G., 1998, MNRAS, 293, L57
Drell, S. D., Foley, H. M., Ruderman, M. A., 1965, J. Geophys. Res., 70, 3131.
Goldreich, P., Lynden-Bell, D., 1969, ApJ, 156, 59
Faulkner, J., 1971, ApJ, 170, L99
Li, J., Ferrario, L., Wickramasinghe, D. T., 1998, ApJ, 503, L151
Motch, C., Haberl, F., Guillout, P., Pakull, M., Reinsch, K., Krautter, J., 1996, A&A, 307, 459
Neubauer, F. M., 1980, J. Geophys. Res., 85, 1171
Paczyński, B., 1967, Acta Astron., 17, 287
Paddington, J. H., Drake, J. F., 1968, Nature 217, 935
Ramsay, G., Cropper, M., Wu, K., Mason, K. O., Hakala, P., 2000a, MNRAS, 311, 75
Ramsay, G., Wu, K., Cropper, M., Schmidt, G., Sekiguchi, K., Iwamuro, F., Maihara, T., 2000b, MNRAS, submitted
Spitzer, L., Härm, R., 1953, Phys. Rev., 89, 977

APPENDIX A: GEOMETRY OF THE HOT SPOTS

Consider a system consisting of a magnetic and a non-magnetic white dwarf in close orbit with a separation a. The magnetic white dwarf has a dipolar field, with the family of field lines given by $r = \mathcal{C}\ \sin^2\theta$, where $\mathcal{C}$ is a constant labeling different field lines. Thus, the geometry of the pole is determined by the field lines that connected the two white dwarfs, and it is specified by the parameter $\tilde{a}$ and $\tilde{b}$, where

$$\begin{aligned}\tilde{a} &= \frac{R_1}{2}\sin\theta\Delta\phi \\ &= \left(\frac{R_1^3}{a}\right)^{1/2}\tan^{-1}\left(\frac{R_2}{a}\right) , \qquad (14)\end{aligned}$$

$$\begin{aligned}\tilde{b} &= \frac{R_1}{2}\Delta\theta \\ &= \frac{R_1}{2}\left(\theta^- - \theta^+\right) \\ &= \frac{R_1}{2}\left\{\sin^{-1}\sqrt{\frac{R_1}{a-R_2}} - \sin^{-1}\sqrt{\frac{R_1}{a+R_2}}\right\} \qquad (15)\end{aligned}$$

(see Figure 5, top and second panels).

If the radius of the stars R_2 and R_1 are significantly smaller than the orbital separation a, then $\tilde{a} \approx R_2(R_1/a)^{3/2}$ and $\tilde{b} \approx (R_2/2)(R_1/a)^{3/2}$. It follows that $\tilde{b}/\tilde{a}$ is approximately 0.5 for a wide range of orbital parameters. Moreover, the fractional area of the dissipative region on the white-dwarf surface $f < (\tilde{a}\tilde{b}/R_1^2) \ll 1$.

APPENDIX B: RESISTIVE DISSIPATION IN THE TWO WHITE DWARFS

For the non-magnetic white dwarf, the conductivity of the core $\sigma_{\rm co}$ is much larger than the conductivity of the atmosphere σ_2 (i.e. $\sigma_{\rm co} \gg \sigma_2$), so that most resistivity dissipation occurs at the atmospheric layer (See Figure 5, bottom panel). The rate of energy dissipation is therefore

$$\begin{aligned}W_2 &= \int_{R_2-\Delta R_2}^{R_2} d^3x\ \left(\vec{J}_2\cdot\vec{E}\right) \\ &= \int_{R_2-\Delta R_2}^{R_2} d^3x\ \frac{1}{\sigma_2}|\vec{J}_2|^2 . \qquad (16)\end{aligned}$$

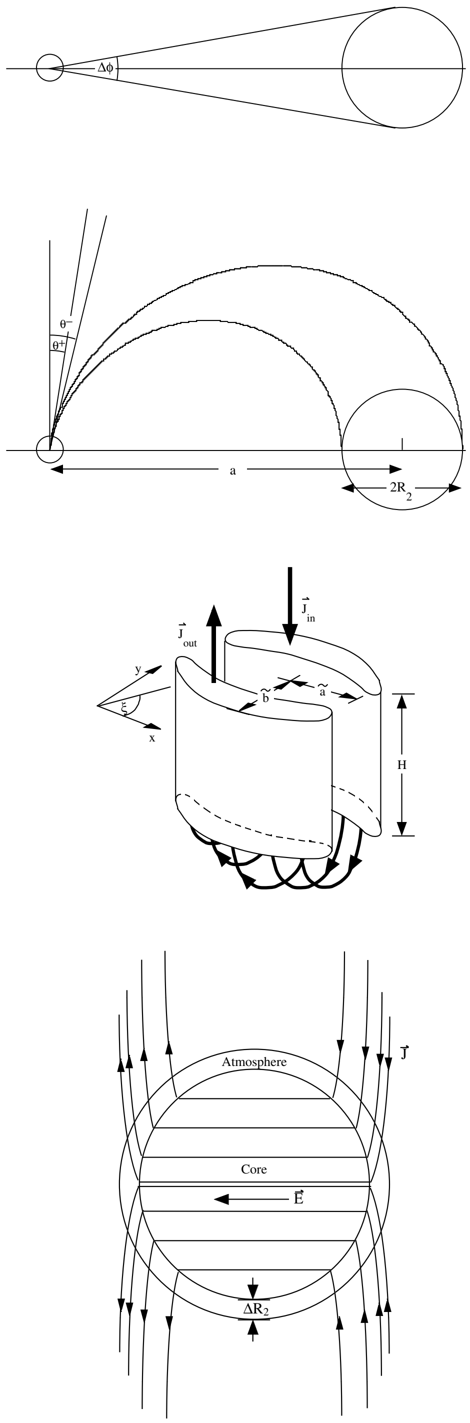

Figure 5. (Top and second panels) The top and side elevation views of the system showing how maximum height and width of the hot spot ($2\tilde{b}$ and $2\tilde{a}$ respectively) at the surface of the magnetic white dwarf are determined. (Third penal) Schematic illustration of the current sheets in the atmosphere of the magnetic primary white dwarf. At depth H below the white-dwarf, collisions are efficient enough to allow the current to cross the magnetic-field lines. Bottom panel) Schematic illustration of the current flow in the non-magnetic secondary white dwarf.

If the current density $\vec{J}$ is roughly homogeneous, then

$$
\begin{aligned}
W_2 &= 4\pi R_2^2 \Delta R_2 \frac{J_2^2}{\sigma_2} \\
&\approx \frac{4}{\pi}\frac{I^2}{\sigma_2 R_2}\left(\frac{\Delta R_2}{R_2}\right) ,
\end{aligned}
\tag{17}
$$

where $I = \pi R_2^2 J_2$ is the current flowing across the star.

For the magnetic white dwarf, the dissipation at each polar spot is

$$
W_1^{(1)} = \int_{\rm spot} d^3x \, \left(\vec{J}_1 \cdot \vec{E}\right) . \tag{18}
$$

It is not trivial to determine the functional form of the current density $\vec{J}_1(\vec{x})$ at the pole. For simplicity, we follow Li, Wickramasinghe and Ferrario (1998) and consider an approximation that the current density is non-zero in two arc-like regions. The thickness of the arc is Δd, and the length and width of the region are $2\tilde{a} = R_1 \sin\theta \Delta\phi$ and $2\tilde{b} = R_1 \Delta\theta$, where θ is the colatitude of the centre of the hot spot. The current density is given by $J_1 = J_{1o}\sin\xi$ (Figure 5, third panel). We assume that at a depth $H(\ll R_1)$ the Pendersen conductivity (see Alfvén & Fälthammar 1963) becomes sufficient large to allow the current to cross the field lines and close the circuits.

The current flowing through the spot is therefore

$$
\begin{aligned}
I &= \int_{\rm spot} dxdy \; J_1 \\
&= J_{1o}(4\tilde{a}\Delta d)\int_0^{\pi/2} d\xi \; \mathcal{Q}_1(\xi; e) ,
\end{aligned}
\tag{19}
$$

and the resistive dissipation is

$$
W_1^{(1)} = \frac{J_{1o}^2}{\sigma_1}(4\tilde{a}H\Delta d)\int_0^{\pi/2} d\xi \; \mathcal{Q}_2(\xi; e) . \tag{20}
$$

The function $\mathcal{Q}_n$ is given by

$$
\mathcal{Q}_n(\xi; e) = \sin^n\xi\sqrt{1-e^2\cos^2\xi} , \tag{21}
$$

where $e = \sqrt{1-(\tilde{b}/\tilde{a})^2}$.

Using the expression for $\tilde{a}$ in Appendix A, we obtain the rate of total dissipation at the magnetic white dwarf:

$$
\begin{aligned}
W_1 &= 2W_1^{(1)} \\
&\approx \frac{1}{2}\frac{I^2}{\sigma_1}\left(\frac{H}{\Delta d}\right)\left(\frac{a}{R_1}\right)^{3/2}\frac{\mathcal{J}(e)}{R_2} ,
\end{aligned}
\tag{22}
$$

where

$$
\begin{aligned}
\mathcal{J}(e) &= \frac{\int_0^{\pi/2} d\xi \; \mathcal{Q}_2(\xi; e)}{\left[\int_0^{\pi/2} d\xi \; \mathcal{Q}_1(\xi; e)\right]^2} \\
&= \pi\left\{1-\sum_{n=1}^{\infty}\left[\frac{(2n-1)!!}{(2n)!!}\right]^2\frac{e^{2n}}{(n+1)(2n-1)}\right\} \\
&\quad \times\left[\sqrt{1-e^2}+\frac{1}{e}\sin^{-1}e\right]^{-2} .
\end{aligned}
\tag{23}
$$

The ratio of the dissipation rates at the two white dwarfs is therefore

$$
\frac{W_1}{W_2} = \frac{\pi}{8}\mathcal{J}(e)\left(\frac{\sigma_2}{\sigma_1}\right)\left(\frac{H}{\Delta d}\right)\left(\frac{R_2}{\Delta R_2}\right)\left(\frac{a}{R_1}\right)^{3/2} . \tag{24}
$$

The exact values of H and Δd are uncertain. Li, Wickramasinghe & Ferrario (1998) argued that roughly $H \sim \Delta d$. As $\sigma_2 \sim \sigma_1$, $\pi\mathcal{J}(e)/8 \sim \mathcal{O}(1)$ and $(R_2/\Delta R_2)(a/R_1)^{3/2} \gg 1$, most of the electric energy will be dissipated at the two hot polar spots of the magnetic white dwarf.

APPENDIX C: ENERGY CONSERVATION

Consider a system with two gravitationally bound, rotating objects, with moments of inertia I_1 and I_2, in circular motion around each other. Let the angular speeds of their rotation be ω_1 and ω_2 respectively. The total mechanical energy of the system is

$$
E = \frac{1}{2}I_1\omega_1^2 + \frac{1}{2}I_2\omega_2^2 + (T+V) . \tag{25}
$$

T and V are the kinetic and potential energy of the orbit, which are related by

$$
\begin{aligned}
T &= \frac{1}{2}I_o\omega_o^2 \\
&= \frac{1}{2}\frac{GM_1^2 q}{a} \\
&= -\frac{1}{2}V ,
\end{aligned}
\tag{26}
$$

where the effective moment of inertia of the orbit $I_o = M_1 a^2[q/(1+q)]$ and the orbital angular speed $\omega_o = [GM_1(1+q)/a^3]^{1/2}$.

If the spin of the second object is in perfect synchronism with the orbit (i.e. $\omega_2 = \omega_o$), then

$$
\begin{aligned}
E &= \frac{1}{2}I_1\omega_1^2 - \frac{1}{2}\left[M_1\left(\frac{q}{1+q}\right)a^2 - \frac{2}{5}M_1 q R_2^2\right]\omega_o^2 \\
&= \frac{1}{2}I_1\omega_1^2 - \frac{1}{2}\frac{GM_1^2 q}{a^3}\left[a^2 - \frac{2}{5}(1+q)R_2^2\right] .
\end{aligned}
\tag{27}
$$

(Here, we have assumed that the objects are spherical, so that their moments of inertia is 2/5 of their mass times the square of their radius.) It follows that

$$
\begin{aligned}
\dot{E} &= I_1\omega_1\dot{\omega}_1 - \frac{1}{2}GM_1^2 q\frac{d}{dt}\left[\frac{1}{a} - \frac{2}{5}(1+q)\frac{R_2^2}{a^3}\right] \\
&= I_1\omega_1\dot{\omega}_1 + \frac{1}{2}\frac{GM_1^2 q}{a}\left[1-\frac{6}{5}(1+q)\left(\frac{R_2}{a}\right)^2\right]\left(\frac{\dot{a}}{a}\right) \\
&= I_1\omega_1\dot{\omega}_1 - \frac{1}{2}I_o\omega_o^2\left[1-\frac{6}{5}(1+q)f(\omega_o)\right]\left(\frac{2}{3}\frac{\dot{\omega}_o}{\omega_o}\right) ,
\end{aligned}
\tag{28}
$$

where $f(\omega_o) = \{R_2^3\omega_o^2/[GM_1(1+q)]\}^{2/3}$. If the second object is close to filling its Roche-lobe, then $R_2 \approx a\lambda[q/(1+q)]^{1/3}$, and

$$
\dot{E} \approx I_1\omega_1\dot{\omega}_1 + \frac{1}{2}I_o\omega_o^2\left[1-\frac{6}{5}\lambda^2(1+q)^{1/3}q^{2/3}\right]\left(\frac{\dot{a}}{a}\right) , \tag{29}
$$

where $\lambda = 0.462$. Clearly, when $q < 0.7$, $\lambda^2(1+q)^{1/3}q^{2/3} < 5/6$, and hence the square bracketed term is positive.

APPENDIX D: WORK DONE BY THE DISSIPATIVE TORQUE

The torque that accelerates/decelerates the spin of the object 1 is

$$\vec{\tau} \equiv I_1 \frac{d}{dt}\vec{\omega}_1 \ , \tag{30}$$

and the torque that changes the spin of object 2 and the orbital rotation is

$$\vec{\tau}_{\rm ex} - \vec{\tau} = I_o \frac{d}{dt}\vec{\omega}_o + I_2 \frac{d}{dt}\vec{\omega}_2 + \vec{\omega}_o \frac{d}{dt} I_o \ , \tag{31}$$

where $\tau_{\rm ex}$ is an external torque.

From the definition of the synchronisation $\alpha \equiv \omega_1/\omega_o$, we have

$$\frac{\dot{\alpha}}{\alpha} = \frac{\dot{\omega}_1}{\omega_1} - \frac{\dot{\omega}_o}{\omega_o} \ . \tag{32}$$

The perfect-synchronism condition for object 2 and the orbit implies that

$$\tau_{\rm ex} - \tau = (I_o + I_2)\dot{\omega}_o + \omega_o \dot{I}_o \ . \tag{33}$$

Thus, the timescale for the change in the orbital angular speed is

$$\frac{\dot{\omega}_o}{\omega_o} = K\left[\frac{\tau_{\rm ex}}{(I_o+I_2)\omega_o} - \left(\frac{\alpha I_1}{I_o+I_2}\right)\frac{\dot{\alpha}}{\alpha} - \frac{\dot{I}_o}{(I_o+I_2)}\right] , \tag{34}$$

and the timescale of spin evolution of object 1 is

$$\frac{\dot{\omega}_1}{\omega_1} = K\left[\frac{\tau_{\rm ex}}{(I_o+I_2)\omega_o} + \frac{\dot{\alpha}}{\alpha} - \frac{\dot{I}_o}{(I_o+I_2)}\right] , \tag{35}$$

where $K = [1+\alpha I_1/(I_o+I_2)]^{-1}$. The first term in the square of above expression is due to the synchronisation process, the second term is the contribution of the external torque, and the last term is caused by the readjustment of the orbital separation.

The work done by the (dissipative) synchronisation torque is

$$\begin{aligned} W &= |\vec{\tau}\cdot(\vec{\omega}_o - \vec{\omega}_1)| \\ &= |I_1 \dot{\omega}_1 \omega_o (1-\alpha)| \\ &= \left| I_1 \omega_o^2 \alpha (1-\alpha)\left[\frac{\dot{\alpha}}{\alpha} + \frac{\dot{\omega}_o}{\omega_o}\right]\right| \ . \end{aligned} \tag{36}$$

It is straightforward to show that the work done can also be expressed as follows:

$$\begin{aligned} W = & \left| I_1 \omega_o^2 \alpha (1-\alpha)\left[1 + \frac{\alpha I_1}{I_o+I_2}\right]^{-1} \right. \\ & \left. \times \left[\frac{\tau_{\rm ex}}{(I_o+I_2)\omega_o} + \frac{\dot{\alpha}}{\alpha} - \frac{\dot{I}_o}{(I_o+I_2)}\right]\right| \ . \end{aligned} \tag{37}$$

APPENDIX E: SPIN-ORBIT EVOLUTION

Suppose the energy loss is represented by a dissipative term due to synchronisation torque $\dot{E}_{\rm diss}$ and an additional term $\dot{E}_{\rm ex}$ (e.g. due to gravitational radiation). Then we have

$$\dot{E}_{\rm diss} - \dot{E}_{\rm ex} = I_1 \omega_1 \dot{\omega}_1 + g(\omega_o)\left(\frac{\dot{\omega}_o}{\omega_o}\right) , \tag{38}$$

where

$$\begin{aligned} g(\omega_o) = & -\frac{1}{3}\left[\frac{q^3}{(1+q)} G^2 M_1^5 \omega_o^2\right]^{1/3} \\ & \times \left[1 - \frac{6}{5}(1+q) f(\omega_o)\right] \ . \end{aligned} \tag{39}$$

The functional form $f(\omega_o)$ can be found in Appendix C. For dissipative synchronisation torque proportional to $(\vec{\omega}_o - \vec{\omega}_1)$, we have

$$\begin{aligned} \dot{E}_{\rm diss} &= -W \\ &= -(1-\alpha) I_1 \omega_o \dot{\omega}_1 \ . \end{aligned} \tag{40}$$

It can be shown that the evolution of the spin of the magnetic white dwarf and the orbital rotation are determined by the following equations:

$$\frac{\dot{\omega}_o}{\omega_o} = \frac{1}{g(\omega_o)}\left[\dot{E}_{\rm ex} - \frac{W}{(1-\alpha)}\right] ; \tag{41}$$

$$\frac{\dot{\alpha}}{\alpha} = -\frac{1}{g(\omega_o)}\left[\dot{E}_{\rm ex} - \frac{W}{(1-\alpha)}\left(1 + \frac{g(\omega_o)}{\alpha I_1 \omega_o^2}\right)\right] \ . \tag{42}$$